In-situ wavelength calibration system for the X-ray Imaging Crystal Spectrometer (XICS) on W7-X[a)]

J. Kring,[1, b)] N. Pablant,[2] A. Langenberg,[3] J. Rice,[4] L. Delgado-Aparicio,[2] D. Maurer,[1] P. Traverso,[1] M. Bitter,[2] K. Hill,[2] and M. Reinke[2]

[1)] *Auburn University, Auburn, Alabama, USA*

[2)] *Princeton Plasma Physics Laboratory, Princeton, New Jersey, USA*

[3)] *Max-Planck-Institut für Plasmaphysik, Greifswald, Germany*

[4)] *Plasma Science Fusion Center, Massachusetts Institue of Technology, Cambridge, Massachusetts, USA*

(Dated: 26 November 2018)

An in-situ wavelength calibration system for the X-ray Imaging Crystal Spectrometer (XICS) on W7-X has been developed to provide routine calibration between plasma shots. XICS is able to determine plasma flow profiles by measuring the Doppler shift of x-ray line emission from high charged impurity species. A novel design is described that uses an x-ray tube with a cadmium anode placed in front of the diffracting spherically bent crystal. This arrangement provides calibration lines over the full detector extent for both the Ar^{16+} and Ar^{17+}/Fe^{24+} spectrometer channels. This calibration system can provide a relative wavelength accuracy of 3×10^{-7} Å across the full spacial extent of the detector, which corresponds to 50 m/s in the W7-X system. An absolute wavelength calibration of 1×10^{-5} Å is expected, corresponding to 1 km/s, based on the current known accuracy of the calibration wavelength and the achievable measurement of the absolute positioning of the hardware. This calibration system can be used to independently calibrate XICS systems on both stellarators and tokamaks, without the need for special plasma conditions often used for calibration, such as locked modes on tokamaks. Experimental and simulated results are shown along with expected results and a complete design of the calibration hardware to be installed in W7-X XICS system.

Keywords: W7-X, XICS, wavelength calibration, radial electric field, impurity transport

I. INTRODUCTION

X-ray Imaging Crystal Spectrometers (XICS) detect the emission of highly charged impurity ions to provide ion temperature, electron temperature, plasma flow velocity, and impurity ion density profiles. XICS systems have been used on W7-X[1], LHD[2], Alcator C-Mod[3], EAST[4], KSTAR and other experiments with a XICS system planned for ITER[5]. The ion temperature is found from the Doppler broadening of spectral lines; the electron temperature from the ratio of different lines; the flow velocity from the Doppler shift of the lines; and the impurity ion density from the line intensities. In a stellarator, the radial electric field, E_r, can be inferred through measurements of the perpendicular plasma flow, $u_\perp$[6]. Measured E_r profiles are important for many aspects of stellarator physics including the study of neoclassical optimization in W7-X. Existing XICS systems lack any independent wavelength calibration capability. On tokamaks, plasma flow measurements are calibrated using locked mode plasma, or through reversing the plasma flow. However, on stellarators, locked mode plasmas are not available. This paper presents an independent, robust calibration design that will work for any XICS system independent of the experiment.

[a)] Contributed paper, published as part of the Proceedings of the 22nd Topical Conference on High-Temperature Plasma Diagnostics, San Diego, California, USA, April 2018.

[b)] Electronic mail: jdk0026@auburn.edu

II. XICS WAVELENGTH CALIBRATION SYSTEM

A. XICS Overview

XICS systems use spherically bent crystals to diffract x-rays to photon counting imaging detectors. The spectral resolution of the diagnostic is produced by the crystals diffracting light of different wavelengths at different angles according to Bragg's Law. The spatial resolution come from the spherically bent shape of the crystal. The W7-X XICS diagnostic consists of two channels utilizing two quartz crystals which measure the Ar^{16+} and Ar^{17+}/Fe^{24+} spectra respectively. In particular, the Ar^{16+} channel utilizes a Quartz (11-20) crystal with a radius of curvature of 1450 mm.

Referenced above, XICS on W7-X is used to infer the radial electric field, E_r, from the perpendicular plasma flow, $u_\perp$. The measurement resolution of the perpendicular plasma flow, when ignoring systematic errors, is $\Delta u_\perp = 1km/s$ ($\Delta E_r = 2kV/m$) with typical levels of argon puffing and a $10ms$ integration time. This corresponds to a shift of the line on the detector by about $5\mu m$. Better resolution is available through additional time binning. The primary systematic errors in these measurements are due to the absolute wavelength calibration across the detector, which in this system, is equivalent to the absolute spacial alignment between the crystal and the detector. The absolute alignment can be considered in two parts: a constant shift across the detector, and a tilt of the detector leading to a linear shift

of the wavelength. Without an absolute wavelength reference, calibration is based on the ability to see a portion of the plasma on both sides of the magnetic axis and the assumption that the parallel velocity is negligible.

Changes in the absolute wavelength calibration are expected to occur at least on the timescale of thermal changes in the diagnostic or the surrounding environment. Only a few degrees of temperature change, similar to what can be expected from an air conditioning cycle, have been shown to cause thermal expansion of the crystal lattice structure and therefore lead to spectral line shifts on the order of the desired plasma flow measurements[7]. Similarly, thermal expansion of the steel structures that the crystal and detector and mounted on are also on the order to potentially cause significant calibration changes. Measurements of the crystal temperature and repeated calibrations during the planned long pulse discharges can be used to compensate for any spectral line shifts due to thermal expansion.

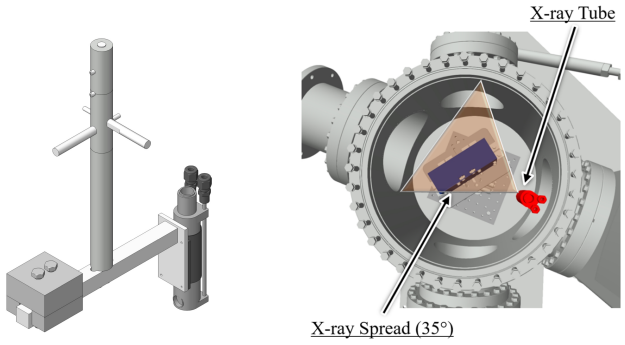

(a) Assembled Design (b) X-ray tube placement

FIG. 1: Assembled calibration design along with the placement of the x-ray tube in the crystal chamber

B. Calibration System Hardware

The wavelength calibration system designed for XICS consists of a x-ray tube positioned in front of the diffracting spherical crystal in order to provide x-ray calibration lines. The specific x-ray lines produced by the chosen anode for the x-ray tube will match the system's spectral range. This wavelength calibration design will illuminate all spacial channels on the detector simultaneously. The full spacial illumination is achieved by positioning the x-ray tube close to spherical crystal and inside the focal points of the spherical crystal. A discussion on the modeling and experimental testing of this setup is covered later on in this paper.

The x-ray tube for this calibration system is the XRT 30 by PROTO Manufacturing Inc. A Cadmium anode on the x-ray tube will provide the Cd $L\alpha$ and Cd $L\beta$ lines needed to calibrate the Ar^{16+} and Ar^{17+}/Fe^{24+} channels respectively for XICS. The x-ray tube will be operated up to 15KeV and 2 mA. It will be placed 100mm from the crystals, between the crystals and the plasma. For routine operation between discharges or during long discharges, the x-ray tube is mounted on a rotating arm attached to a standard rotary feedthrough with fine motion control. This setup allows the x-ray tube to be easily rotated in and out of the line of sight of the spherical crystals.

The assembled calibration design is pictured in Figure 1. For simplicity, the flanges, nipples, feedthroughs, cooling lines, and cabling have been hidden from rendering in Figure 1. The vertical shaft pictured connects the rotary feedthrough to the rotating arm holding the x-ray tube in addition to a counterweight balancing the x-ray tube. The two arms extending from the upper middle portion of the vertical shaft are physical safety stopping arms that prevent the x-ray tube from being positioned such that x-rays would enter the W7-X experiment. A post fastened to the top flange is the non-rendered component that will limit the motion of the arms.

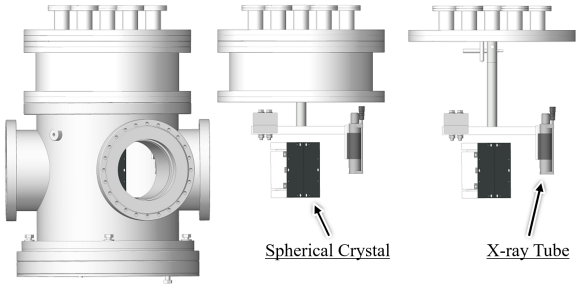

FIG. 2: The placement of the x-ray tube with respect to the crystal chamber

Figure 2 shows how the calibration system will replace the top flange on the chamber that houses the crystal. On the left, the crystal chamber is shown with new addition placed on top. Progressing to the right in Figure 2, the location of the calibration design can be seen with respect to the spherical crystal. Shown here, the x-ray tube is in the active position required for illumination of one of the detector channels. The system can be rotated to place the x-ray tube in position for the second crystal. In the stored position, the x-ray tube will be rotated behind the crystal and will not limit any current capabilities of the XICS system. Extra ports have been put on the top flange to allow the installation of a camera to insure the rotary system is functioning properly.

Figure 3 shows the placement of the X-ray tube in relation to the crystal and the plasma. This top-mounted arrangement of the x-ray tube in the chamber holding the crystal allows convenient access for installation and maintenance of the wavelength calibration system.

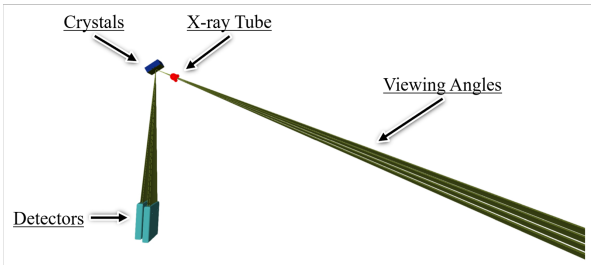

FIG. 3: X-ray tube placement compared to the viewing angles of XICS

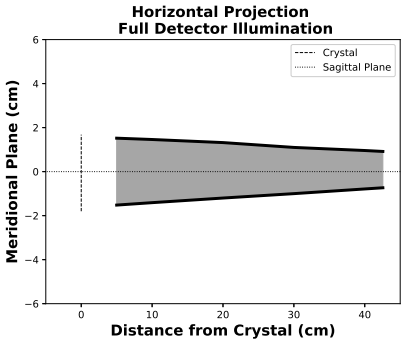

FIG. 4: Horizontal projection of the configuration envelope

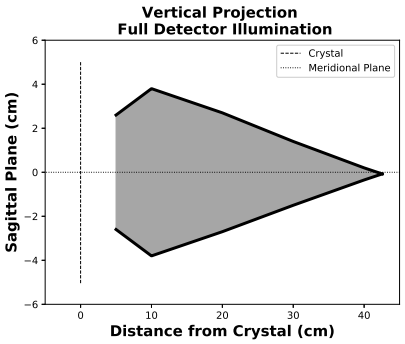

FIG. 5: Vertical projection of the configuration envelope

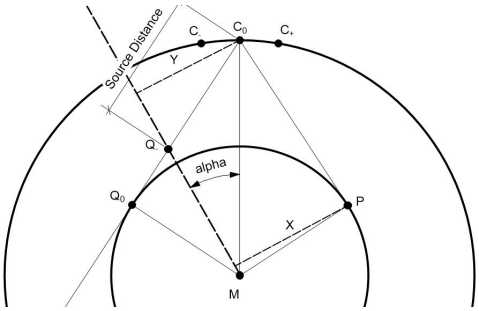

FIG. 6: Two-dimensional projection (top down view) of the XICS geometry

III. SIMULATION & MODELING

A. X-ray Ray Tracing

In order to validate the calibration design, X-ray Imaging Crystal Spectrometer Ray Tracing (XICS-RT) was developed as a tool to analyze and test the proposed design. XICS-RT is an object-oriented, ray tracing code written in Python that simulates the x-ray source, the spherical crystal, and the detector. The rays of a desired wavelength are generated with a random direction inside a cone defined by the spread of the source. The rays are propagated to the crystal location, and only those satisfying the Bragg condition are diffracted toward the detector. The detector counts all incident rays and outputs a TIF image file.

Using XICS-RT with the actual geometry of the XICS system on W7-X coupled with the physical characteristics of the x-ray source, the available configuration space for positioning the x-ray tube such that the detectors are illuminated over the full vertical extent was determined. Figures 4 and 5 respectively show the horizontal and vertical projections of the configuration space. If the x-ray source is positioned anywhere inside this configuration envelope and directed at the spherical crystal, then the full vertical extent of the detector will be illuminated. The optimal position is along the center of the configuration envelopes.

B. Analytical Formulation

XICS-RT was verified using an analytic formulation that was developed to understand the geometry of a spherical crystal x-ray spectrometer. Figure 6 shows this geometry. The two circles represent spheres having radii of R and $R\,cos\,\theta_B$ with R being the radius of curvature of the spherical crystal and θ_B the Bragg Angle. The crystal's width extends from C_- to C_+ with C_0 being the center of the crystal. M is the center of curvature of the crystal, and P is the location of the planar detector. The rays, which are incident on the center of the crystal and diffracted according to the Bragg angle θ_B must be tangential to the sphere with radius $R\,cos\,\theta_B$. In order to satisfy the Bragg condition at the center of the spherical crystal, the source must lie on the $\overline{C_0 Q_0}$ line. For practical considerations, the source is inside the Q_0 position at some arbitrary Q_- location.

With the source located inside the focal lengths of the crystal, the resulting image on the detector is produced from a virtual image. The location of the virtual image (not shown in Figure 6) is at the intersection of the lines $\overline{Q_- M}$ and $\overline{PC_0}$. With this virtual image, a characterization of the detector image can be made by rotating all rays which satisfy the Bragg angle about the $\overline{Q_- M}$ axis.

Using the actual geometry of XICS, Figure 7 shows the comparison of XICS-RT to the analytical formulation. In Figure 7, the vertical extent of the detector refers to the height of the planar detector that is illuminated by

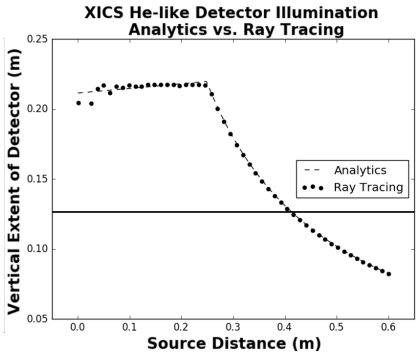

FIG. 7: Comparison of XICS-RT and the analytical formulation

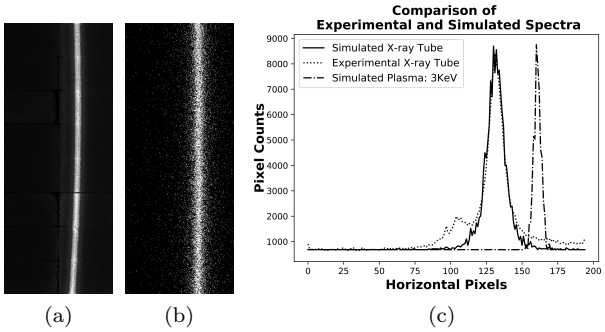

FIG. 8: (a) Experimental and (b) Simulated images of the x-ray tube with profiles compared with simulated plasma light in (c)

an x-ray source positioned at the corresponding location. Any vertical extent above the solid horizontal line (the physical height of the detector) corresponds to the full illumination of all spacial channels on the detector. The plateau region in Figure 7 resulted from the finite width of the detector plane; the decaying region resulted from the fixed spread of the x-ray source (chosen to match the actual x-ray tube). Good agreement was found between XICS-RT and the analytical formulation.

IV. EXPERIMENTAL TESTING

A. Direct Illumination

Testing of the calibration design has been completed at the Plasma Science and Fusion Center (Cambridge, MA) using the High Resolution X-ray Crystal Imaging Spectrometer with Spatial Resolution (HIREXSR, an almost identical system to XICS)[3]. An x-ray tube (same model as one in the calibration design) with a Cadmium anode at 9.5 kV, 0.5 mA was positioned in front of the diffracting crystal at a distance of 4 cm with the angles satisfying the Bragg condition. With an exposure of 500s (acceptable for wavelength calibrations), full illumination of the two working modules of the detector was found.

Figure 8a shows the resulting image from the central module of the detector produced by the Cadmium Lα_1 and Cadmium Lα_2 lines. Figure 8b is the XICS-RT produced image with simulated x-ray source having the same spread, size, and distance from the spherical crystal as the actual experiment but only including the Cd Lα_1 line in the simulation. Figure 8c illustrates the agreement between the two by plotting the vertically-centered, binned rows from each image.

B. Indirect Illumination

In an attempt to identify possible calibration schemes, several indirect illumination calibration methods, were

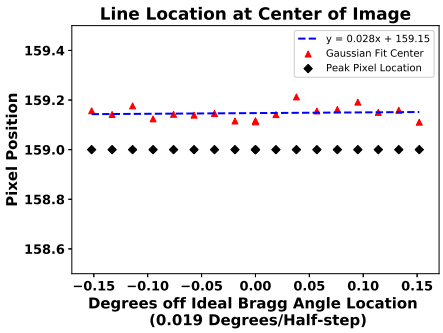

FIG. 9: The impact of the x-ray tube placement on the pixel position of the calibration spectral line

investigated. These methods were motivated in order to provide a calibration source that would use the full crystal surface, mimicking the plasma. For the first test, a Cu x-ray tube was used to illuminate a thick Cadmium sheet in an attempt to excite reflection x-ray fluorescence. With a 2mm thick Cadmium sheet placed approximate 30cm in front of the crystal, the x-ray tube was positioned to the side of the crystal and aimed at the Cadmium sheet such that the illuminated area was in the line of sight of the full crystal. Next, transmission x-ray fluorescence was attempted with a thin $2\mu m$ Cadmium foil, placed 2cm from the crystal between the crystal and the Cu x-ray source. Finally, direct x-ray reflection of a Cd x-ray tube was tested using Cadmium, steel, and carbon sheets as the reflecting surfaces. All attempted methods failed to produce any detectable Cadmium lines on the detector, even after integration times of many hours. The lack of detectable x-ray emission is likely attributable to very small fluorescence yields. The indirect calibration methods were abandoned in favor of direct illumination of the spherical crystal by the x-ray tube as described in this paper.

FIG. 10: XICS-RT produced image of the principle Ar^{16+} line of the plasma

V. WAVELENGTH CALIBRATION ACCURACY

The wavelength calibration accuracy of this design is limited by the random and systematic errors present in the system. The first random error in the wavelength calibration is the positioning of the x-ray tube at optimal Bragg angle location which is dependent upon the rotary feedthrough. Figure 9, the results of a positioning test using XICS-RT, shows the change in position of the spectral lines (both the peak pixel location as well as a Gaussian fit pixel location) with a change in the angular rotation of the rotary feedthrough. Using the slope of the line fit to the Gaussian fit pixel location, the half-step of the rotary feedthrough (0.0019°) corresponds to a spectral shift of 2×10^{-7} Å (0.0005 pixels). Another random error is the ability to fit the spectral lines of the data. From the experimental testing with a 500 s exposure, the fitting error in the location of the calibration line is 1.5×10^{-7} Å (0.0004 pixels). The third possible random error is thermal expansion of the crystal or support system during the calibration exposure time. This limits the maximum integration time that can be used during the calibration, and can be potentially mitigated through characterization of the thermal effects on spectral line shifts coupled with precise temperature measurements.

The first systematic error to be quantified is the precision of the wavelength of the Cadmium lines ($L\alpha$ and $L\beta$) to be used for calibration. A literature study produces the most precise measurements to be 3.95635 ± 0.00004 Å and 3.73823 ± 0.00004 Å respectively[8]. Two additional systematic errors arise because the x-ray tube is much smaller than the plasma and much closer, meaning only a fraction of the crystal will be used to diffract the calibration x-rays (compared to the plasma light using the full crystal). First, this difference will produce a change in the shape of the spectral lines. Second, depending on the location of the x-ray tube, a spectral line shift will also occur. Both of these systematic errors will be modeled using XICS-RT. A high quality correction is expected; however, the final accuracy of this procedure will depend on our ability to accurately characterize the extent and angular spread of the x-ray source, as well as the rocking curve of the crystal. Figure 10 demonstrates XICS-RT's ability to produce plasma spectra (image has been rotated for this paper). This image was generated using a slab Ar^{16+} plasma (only the W-line simulated) at 5KeV placed at the distance of 3.5m from the crystal. Given an absolute position accuracy of 1.5mm (estimated value based on available remote measuring methods for the x-ray tube location relative to the crystal center), an absolute wavelength accuracy of 1×10^{-5} Å (1 km/s) is achievable. The future addition of a collimating slit may allow an in-situ calibration of the position of the x-ray tube with respect to the crystal edges, allowing a significant improvement in the absolute calibration.

VI. CONCLUSION

A wavelength calibration system for x-ray imaging crystal spectrometers using direct illumination of the spherical diffracting crystal has been developed, tested, and designed for XICS on W7-X. This system will provide a wavelength calibration across the whole detector with very high accuracy (limited mainly by integration time), but with a single remaining systematic offset. The random error in the measurement is estimated to be 3×10^{-7} Å (50 m/s) with a systematic error of 1×10^{-5} Å (1 km/s). This greatly improves the ability to measure perpendicular flow profiles to high accuracy, and will allow, for the first time on W7-X, parallel flow velocities to be simultaneously measured up to the larger systematic accuracy. Future improvements of the systematic accuracy are expected from future planned improvements in determination of the absolute location of the x-ray source and cross calibration with other diagnostics.

ACKNOWLEDGEMENTS

Research supported by the U.S. DOE under Contract No. DE-AC02-09CH11466 with Princeton University. This work has been carried out within the framework of the EUROfusion Consortium and has received funding from the Euratom research and training programme 2014-2018 under grant agreement No 633053. The views and opinions expressed herein do not necessarily reflect those of the European Commission. We thank MIT PSFC for the use of their facilities in testing the calibration schemes.

[1] N. Pablant *et al.* *41st EPS Conference on Plasma Physics*, 38F:P1.076, 2014.

[2] N. A. Pablant *et al.* Layout and results from the initial operation of the high-resolution x-ray imaging crystal spectrometer on the large helical device. *Review of Scientific Instruments*, 83(8):083506, 2012.

[3] A. Ince-Cushman *et al.* Spatially resolved high resolution x-ray spectroscopy for magnetically confined fusion plasmas (invited). *Review of Scientific Instruments*, 79(10):10E302, 2008.

[4] B. Lyu *et al.* Measurement of helium-like and hydrogen-like argon spectra using double-crystal x-ray spectrometers on east. *Review of Scientific Instruments*, 87(11):11E326, 2016.

[5] J. Maddox *et al.* Multi-energy x-ray detector calibration for te and impurity density (nz) measurements of mcf plasmas. *Review of Scientific Instruments*, 87(11):11E320, 2016.

[6] N. A. Pablant *et al.* Core radial electric field and transport in wendelstein 7-x plasmas. *Physics of Plasmas*, 25(2):022508, 2018.

[7] L Delgado-Aparicio *et al.* Effects of thermal expansion of the crystal lattice on x-ray crystal spectrometers used for fusion research. *Plasma Physics and Controlled Fusion*, 55(12):125011, 2013.

[8] J.A. Bearden. X-ray wavelengths. *Review of Modern Physics*, pages 86–99, 1967.